

Gas Accretion as a Dominant Formation Mode in Massive Galaxies from the GOODS NICMOS Survey

Christopher J. Conselice^{1*}, Alice Mortlock¹, Asa F.L. Bluck^{1,2}, Ruth Grützbauch¹, Kenneth Duncan¹

¹*University of Nottingham, School of Physics & Astronomy, Nottingham, NG7 2RD UK*

²*Gemini Observatory*

Accepted ; Received ; in original form

ABSTRACT

The ability to resolve all processes which drive galaxy formation is one of the most fundamental goals in extragalactic astronomy. While star formation rates and the merger history are now measured with increasingly high certainty, the role of gas accretion from the intergalactic medium in supplying gas for star formation still remains largely unknown. We present in this paper indirect evidence for the accretion of gas into massive galaxies with initial stellar masses $M_* > 10^{11} M_\odot$ and following the same merger adjusted co-moving number density at lower redshifts during the epoch $1.5 < z < 3$, using results from the GOODS NICMOS Survey (GNS). Our method utilises the observed star formation rates of these massive galaxies based on UV and far-infrared observations, and the amount of stellar and gas mass added due to observed major and minor mergers to calculate the evolution of stellar mass in these systems. We show that the measured gas mass fractions of these massive galaxies are inconsistent with the observed star formation history for the same galaxy population. We further demonstrate that this additional gas mass cannot be accounted for by cold gas delivered through minor and major mergers. We also consider the effects of gas outflows and gas recycling due to stellar evolution in these calculations. We argue that to sustain star formation at the observed rates there must be additional methods for increasing the cold gas mass, and that the likeliest method for establishing this supply of gas is by accretion from the intergalactic medium. We calculate that the average gas mass accretion rate into these massive galaxies between $1.5 < z < 3.0$, is $\dot{M} = 96 \pm 19 M_\odot \text{ yr}^{-1}$ after accounting for outflowing gas. This is similar to what is predicted in detailed simulations of galaxy formation. We show that during this epoch, and for these very massive galaxies, $49 \pm 20\%$ of baryonic mass assembly is a result of gas accretion and unresolved mergers, while the remaining $\sim 25 \pm 10\%$ is put into place through existing stars from mergers, with the remainder is gas brought in with these mergers. However, $66 \pm 20\%$ of all star formation in this epoch is the result of gas accretion. This reveals that for the most massive galaxies at $1.5 < z < 3$ gas accretion is the dominant method for instigating new stellar mass assembly.

Key words: Galaxies: Evolution, Formation, Structure

1 INTRODUCTION

Both observations and theoretical models now overwhelmingly suggest that galaxies have evolved from an early population dominated by lower mass systems undergoing significant star formation in the early universe, to the large and relatively passive galaxies that we find today (e.g., Conselice

2006; Bouwens et al. 2010). How this transformation occurs, that is how we get from young low mass galaxies to the large massive galaxies we see in today’s universe, is a highly debated topic. Essentially, we want to answer the question - how do galaxies assemble their stellar masses? The answer to this question will have profound implications for both the physics of galaxy formation and for understanding properties of the universe itself.

* E-mail: conselice@nottingham.ac.uk

Historically, it was once thought that galaxies formed in

a manner similar to stars through a collapse of gas that later, through some process, underwent intense star formation. In this paradigm the total baryonic mass of a galaxy does not change significantly with time, and its stellar mass evolves by rapidly converting gas into stars. However, it is clear that galaxies must form in a hierarchical way through mergers and accretion of material from the intergalactic medium. This view has supporting evidence from both observations of the stellar mass functions of galaxies (e.g., Bundy et al. 2006; Mortlock et al. 2011), direct observations of mergers in the distant universe (e.g., Conselice et al. 2003, 2008; Bluck et al. 2009, 2012), as well as through the evolution of galaxy sizes (e.g., Ferguson et al. 2004; Trujillo et al. 2007; Buitrago et al. 2008; Weinzirl et al. 2011). Evidence from internal kinematics also suggests that galaxy formation is driven at least in part by the accumulation of gas from the intergalactic medium falling onto a galaxy (e.g., Keres et al. 2005; Genzel et al. 2008; Dekel et al. 2009a,b; Bournaud et al. 2011).

While it is now generally accepted that galaxy formation is a hierarchical process driven by the accumulation of stars and gas located outside of a galaxy after its initial formation, the details of this assembly remain largely unknown. Cold gas infall into galaxies, otherwise known as ‘cold gas accretion’ is theorised to be an important aspect in the process of massive galaxy formation (e.g., White & Frenk 1991; Birnboim & Dekel 2003; Keres et al. 2005, Dekel et al. 2009a,b), and even perhaps the dominant method by which galaxies assemble their mass. However, there is little to no evidence for gas accretion onto galaxies at high redshift currently (e.g., Steidel et al. 2010), although some claims are appearing at lower redshifts (e.g., Rauch et al. 2011). This is primarily due to the difficulty of observing this process since the covering fraction of accreting cold gas is likely not high (e.g., Faucher-Giguere, Keres & Ma 2011; Kimm et al. 2011; Fumagalli et al. 2011), nor would this gas be easily detected in, for example, absorption (e.g., Weiner et al. 2009; Giavalisco et al. 2011).

In this paper we develop a new approach to this problem by analyzing the evolution of the massive galaxy population in terms of the history of its baryonic assembly. We examine how the stellar mass of a massive galaxy is built up during $1.5 < z < 3$ through various galaxy formation processes observed within a unique sample of $M_* > 10^{11} M_\odot$ galaxies taken from the GOODS NICMOS Survey (GNS) (Conselice et al. 2011). By examining the addition of stellar mass due to major and minor mergers (Bluck et al. 2009; 2012), and the observed star formation history (Bauer et al. 2011) and resulting stellar mass evolution using stellar synthesis modeling, we provide through this method circumstantial evidence for gas inflow, or gas imported in through extremely minor mergers, as an important process in galaxy assembly.

After comparing the amount of accreted mass to the mass assembled through merging, we conclude that gas accretion is a dominant process for massive galaxy assembly at this epoch. We further discuss the comparison with theory, and describe some of the implications of our results, including how our work relates to the G-dwarf problem (e.g., Larson 1974), and the rapid gas depletion time-scales in galaxies.

This paper is organised as follows: §2 includes a discussion of the data sources we use in this paper, and the sample

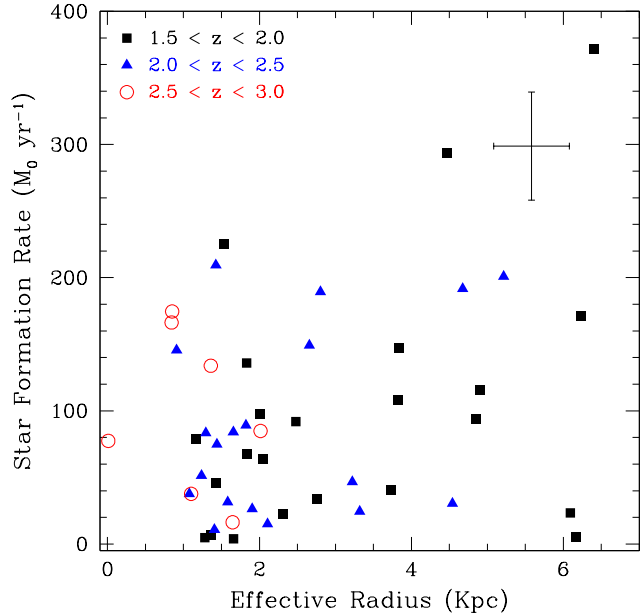


Figure 1. The relationship between the star formation rate and effective radius, R_e , divided into three redshift ranges between $1.5 < z < 3$ for galaxies with stellar masses $M_* > 10^{11} M_\odot$.

selection, §3 is a description of our baryonic mass assembly analysis, §4 presents our arguments for gas accretion and §5 is our summary. We use a standard cosmology of $H_0 = 70 \text{ km s}^{-1} \text{ Mpc}^{-1}$, and $\Omega_m = 1 - \Omega_\lambda = 0.3$ throughout.

2 DATA, DATA PRODUCTS AND GALAXY SELECTION

2.1 Data Sources

The data and methods we use in this paper originate from the GOODS NICMOS Survey (GNS), and are described in detail in Conselice et al. (2011), Mortlock et al. (2011), Bluck et al. (2009, 2012) and Bauer et al. (2011). The primary galaxies and parent sample we examine are 81 massive galaxies with stellar masses $M_* > 10^{11} M_\odot$ at redshifts $1.5 < z < 3$. These were selected through a variety of colour selections, include Distant Red Galaxies (DRGs), IRAC Extremely Red Objects (IEROs) and the BzK selected systems (Conselice et al. 2011). We also utilise photometric redshifts which are described in detail in Grützbauch et al. (2011a,b).

To calculate stellar masses we use a Bayesian method to fit spectral energy distributions based on various star formation models to the galaxy photometry. The distribution of the resulting stellar masses gives us an error in their measurement, and we take the peak value of the distribution as a measure of our stellar mass. A Salpeter IMF was used in these calculations. Further details about our sample se-

lected are included in Conselice et al. (2011) where we refer interested readers for more details.

The galaxy effective radii which we use in this study to measure star formation rate surface densities, originate from GALFIT fits to our NICMOS imaging, taken from the methods and catalog of Buitrago et al. (2008, 2011). These are single Sérsic profile fits to the light profile in which we retrieve both a Sérsic index, n , as well as the effective radius, R_e . These sizes are measured solely using the GOODS NICMOS Survey H_{160} -band imaging. Detailed simulations show that we are able to retrieve these parameters given the observing conditions of our sample (Buitrago et al. 2011).

We also utilise results from previously published GNS studies which describe the evolution of this sample in terms of the star formation rate (Bauer et al. 2011) and the merger history (Bluck et al. 2009; 2012) as a function of stellar mass. We give brief summaries of these analyses in reference to our current study throughout this paper. The star formation rates we use for our galaxies are measured through rest-frame UV and Spitzer 24 μm measurements, which are consistent with each other (Hilton et al. 2012). For the UV star formation rates, which are used for most of the analysis here, we utilise ACS z-band imaging to obtain a rest-frame UV flux measurement which is converted to a star formation rate after applying a k-correction (Bauer et al. 2011). We further measure the UV slope for each galaxy using the UV colour to correct for dust extinction.

2.2 Galaxy Selection

Our galaxy sample is initially chosen simply as all systems within our sample which have stellar masses of $M_* > 10^{11} M_\odot$ at redshifts of $2.75 < z < 3$. We select all galaxies within these limits, including passive galaxies or star forming galaxies. Our range of star formation measures for our massive galaxies include systems that would be identified by colours as passive, but which still have measurable star formation rates, albeit not as high as more active systems. In fact, the star formation rates measured for our sample range from less than $10 M_\odot \text{ year}^{-1}$ to over $300 M_\odot \text{ year}^{-1}$, with a small fraction of 5% of systems having a star formation rate too low to measure.

We include all of the galaxies in our co-moving number density selection as the star formation rate and gas mass fractions we use are an average within this population. The resulting conclusions are therefore valid for the ‘average’ galaxy within our selection. We assume that our sample of galaxies represents different phases of a massive galaxy’s lifespan throughout the redshifts $1.5 < z < 3$. For example, the fraction of galaxies which are passive represents the fraction of time a typical galaxy in our sample is not undergoing star formation. Our sample of galaxies all have very similar stellar masses and environments, suggesting that these systems should have similar formation histories (e.g., Grützbauch et al. 2011a,b). The result of this is that we can obtain the average amount of stellar mass added to this sample selection due to star formation and merging without having to worry about biases from different evolutionary phases.

One issue that we have to account for is that the initial selection of $M_* > 10^{11} M_\odot$ at redshifts of $2.75 < z < 3$ cannot be traced at a constant mass limit. In Conselice et al. (2011) and Mortlock et al. (2011) we discuss the stellar mass

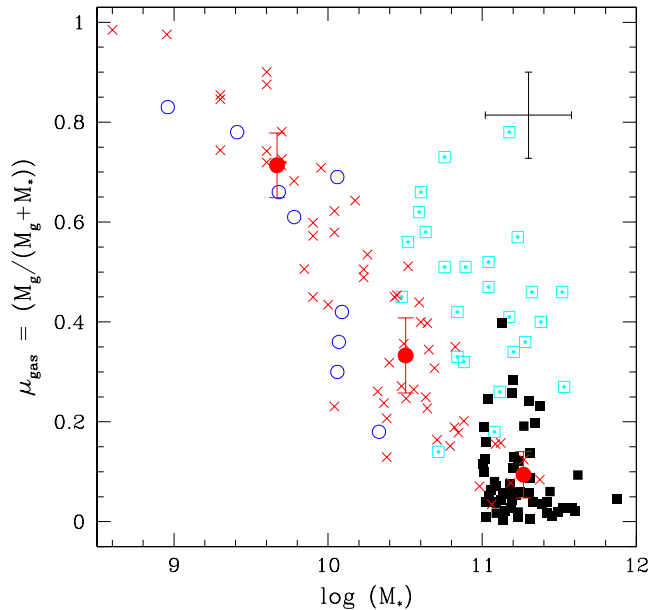


Figure 2. The relation between stellar mass (M_*) and the gas mass fraction μ_{gas} , which is the ratio of the cold gas mass divided by the stellar+gas mass. The red crosses are for $z > 2$ galaxies from Erb et al. (2006) and the blue circles are from Mannucci et al. (2009). The solid black boxes are from the GNS (this work). The error bars show the averages and the 1σ dispersion as a function of stellar mass. The cyan points with square boxes are the CO measurements of starbursting galaxies at similar redshifts from Daddi et al. (2010) and Tacconi et al. (2010).

evolution for our sample. By examining our mass selection used in this paper we find that the number density of galaxies selected by the criterion $M_* > 10^{11} M_\odot$ grows by a factor of between two and four from redshifts $z = 3$ to $z = 1.5$. We therefore examine in this paper our galaxy sample at a constant merger adjusted co-moving number density, taking account of both mergers and star formation which changes the stellar masses of our initially selected galaxies and those below our initial mass limit.

We find that starting with a mass range of $\log M_* > 11$ at $2.5 < z < 3$ due to changes in star formation and merging (Bluck et al. 2012) this mass limit grows to $\log M_* = 11.2$ at redshifts $2.0 < z < 2.5$ and $\log M_* = 11.3$ at $1.5 < z < 2$. Overall on average a galaxy will undergo around a single major merger, thereby decreasing the number of systems in our initial selection during this epoch. We account for this by tracing at a resulting decreased number density to follow the same original galaxies.

Figure 1 shows a summary plot of our data and massive galaxy sample. Plotted are the star formation rates vs. the effective radii for each galaxy in our sample, divided into different redshift bins. The average star formation rate for our sample is roughly constant with redshift (Bauer et al. 2011), and there is a slight evolution in the sizes of these galaxies, such that they are growing with time (e.g., Buitrago et al. 2008).

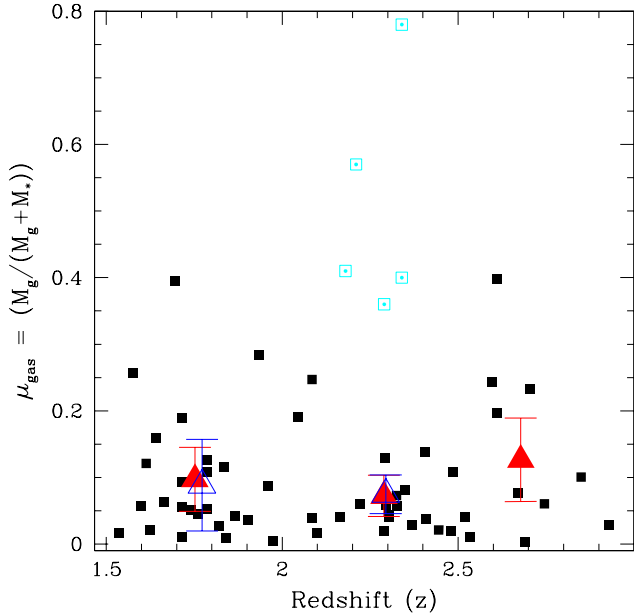


Figure 3. The relation between the gas mass fraction and redshift for galaxies with stellar masses $M_* > 10^{11} M_{\odot}$. The error bars show the 1σ scatter for the average values which are plotted as large solid triangles. The red triangles are for this method when examining galaxies at a stellar mass cut off of $\log M_* > 11$, and the open blue triangles are when holding at a constant merger adjusted co-moving number density to account for more galaxies entering our mass selection over time. The cyan points surrounded by boxes are the galaxies from Daddi et al. (2010) and Tacconi et al. (2010) which meet our stellar mass criteria.

3 EVOLUTION OF GALAXY MASS

3.1 Galaxy Gaseous Mass at $z > 1.5$

The evolution of the cold gas mass within galaxies is an important aspect for understanding galaxy evolution, yet our observations of this quantity are still very basic and are prone to systematic errors. Furthermore, all of these measurements are indirect, even when using CO as a proxy. We present in this section arguments for how to quantify gas masses in our galaxy sample based on the inverse Schmidt-Kennicutt relation (e.g., Kennicutt 1998; Erb et al. 2006; Daddi et al. 2010; Boquien et al. 2012) using our measured SFRs and sizes (Bauer et al. 2011, Buitrago et al. 2011; §2).

Obtaining a measure of the cold gas mass in galaxies is challenging, and there are several attempts to measure this at high redshift (e.g., Erb et al. 2006; Mannucci et al. 2009; Daddi et al. 2010), yet these methods contain several important limitations which must be considered. These inferred cold gas mass fractions are measured through the inverse Schmidt-Kennicutt relation, which relates the cold gas mass surface density to the star formation rate surface density (e.g., Kennicutt 1998). This relation, for nearby galaxies, has been studied in detail in recent papers such as Bigiel et al. (2011) who find a significant scatter, but still a cor-

relation, between these two quantities using molecular gas and star formation measurements. Much of this scatter is however proposed by Krumholz et al. (2012) to be due to observational projection effects, and that there is a universal star formation-gas surface density law that applies at all redshifts (see also Narayanan et al. 2011). There is also evidence that at least two star formation laws may apply at higher redshifts, one for disk-like galaxies, and another for starbursts (e.g., Bouche et al. 2007; Daddi et al. 2010; Genzel et al. 2010).

Most high- z observations, including ones based on CO detections, argue that the cold gas mass fraction, M_{g}/M_* is between 10-50% for galaxies more massive than $M_* = 10^{10} M_{\odot}$ (e.g., Genzel et al. 2010; Daddi et al. 2010; Figure 2). This cold gas mass fraction tends to rise for lower mass galaxies (e.g., Erb et al. 2006; Mannucci et al. 2009). There is also evidence that the efficiency of star formation within starbursts, such as ULIRGs and sub-mm galaxies is more efficient than that given by the standard Schmidt-Kennicutt law, resulting in lower derived gas mass fractions at a measured star formation rate surface density (e.g., Daddi et al. 2010; Boquien et al. 2012).

We calculate gas masses for our massive $M_* > 10^{11} M_{\odot}$ sample, and derive the cold gas mass fraction using a form of the global Schmidt-Kennicutt law calibrated for nearby star forming galaxies. The relation we use is:

$$\Sigma_{\text{SFR}} = (2.5 \pm 0.7) \times 10^{-4} \left(\frac{\Sigma_{\text{gas}}}{1 M_{\odot} \text{pc}^{-2}} \right)^{1.4 \pm 0.15} M_{\odot} \text{yr}^{-1} \text{kpc}^{-2}, \quad (1)$$

where Σ_{SFR} is the surface density of star formation, and Σ_{gas} is the surface density of cold gas. We assume in this calculation that the star formation follows the distribution of H-band light, which is found to be the case (Ownsworth et al. 2012). In any case the exact form of the profile in star formation and light are not important as long as the effective or half-light radius, R_e , are the same. We calculate the star formation rate surface density within each galaxy based on the effective radius, R_e (§2), and half of the measured total star formation rate. From this we obtain the gas mass surface density using eq. (1) and we then calculate the total gas masses in our systems based on this.

In Figure 2 we plot the gas mass divided by total baryonic mass ($M_* + M_{\text{g}}$) for our sample of massive galaxies. We also show in Figure 2 comparison values from Erb et al. (2006) who study galaxies at similar redshifts, but at lower masses, and Mannucci et al. (2009) who study similar star forming galaxies at $z > 2$. We also plot on Figure 2 and Figure 3 the direct measurements of cold gas masses from Tacconi et al. (2010) and Daddi et al. (2010) who both find gas fractions towards the upper end of our stellar mass selected sample. This is not unexpected given that these two studies measure gas masses for galaxies with the highest star formation rates at these redshifts.

Figure 2 shows that the galaxies in our sample, as plotted by the black boxes, have gas total mass fractions which are around 10%, with some scatter. However, our values are lower than the gas total mass fraction found for lower stellar mass systems, and extend the trend found in Erb et al. (2006) and Mannucci et al. (2009), such that the highest mass systems have the lowest relative gas fractions.

To determine how much more stellar mass these galaxies could acquire from the existing cold gas in star formation

events, we show in Figure 3 the gas mass fraction as a function of redshift. The average of the ratio of the gas mass to stellar mass at the three redshift ranges we examine, and the 1σ dispersions of these ratios are at $z \sim 1.75 - f_g = 0.13$, $\sigma = 0.15$, $z \sim 2.29 - f_g = 0.08$, $\sigma = 0.08$ and at $z \sim 2.68 - f_g = 0.17$, $\sigma = 0.19$.

We compute these averages when we hold our selection at a constant merger adjusted co-moving number density as the open blue triangles on Figure 3. We thus find, as others have (Mannucci et al. 2009), that the gas mass fraction is roughly constant with redshift for both a constant mass selection, and using a constant merger adjusted co-moving number density selection. This is also found by comparing derivations of gas mass fractions at different redshifts for lower mass galaxies (e.g., Erb et al. 2006; Mannucci et al. 2009).

It has been noted in previous studies that the gas masses and depletion times scales are not consistent with the star formation observed in these systems (e.g., Genzel et al. 2010). Figure 4 displays the depletion time-scale, the gas mass divided by the star formation rate (ψ), i.e., M_g/ψ – showing that nearly all galaxies in our parent sample would be depleted of gas in less than 0.5 Gyr assuming 100% efficiency of star formation. This is much less than the time within the redshift interval we examine in this paper. While some of these galaxies may become red/passive systems very quickly, the average galaxy within our co-moving number density selection still contains a high star formation rate. This suggests that something is replenishing the gas within the average galaxy within our selection over time.

3.2 The Evolution of Stellar Mass from Star Formation

Galaxy stellar mass is a measure of both the amount of gas which has been converted into stars over time, as well as the amount of mass which has been accreted into the galaxy from previously existing galaxies. We are able to trace both of these properties for the most massive galaxies in the universe up to $z \sim 3$ (e.g., Conselice et al. 2011; Mortlock et al. 2011; Bauer et al. 2011; Bluck et al. 2012).

The reason we can do this now is that we have constructed a complete sample of massive galaxies at redshifts $z = 1.5$ to $z = 3$ which have stellar masses in excess of $M_* = 10^{11} M_\odot$ (Conselice et al. 2011) that have measured minor+major merger measurements (Bluck et al. 2012). We examine galaxies within this selection at $2.75 < z < 3$ and follow at lower redshifts the same systems by observing galaxies at a constant co-moving merger adjusted number density. Using this method, we are ensuring that we are examining similar galaxies at different redshifts (§2.2).

In previous work, we carried out detailed calculations of the merger and star formation histories for a sample of 81 massive galaxies at $1.5 < z < 3$ (Bauer et al. 2011; Bluck et al. 2012) which we discuss here. We find that the average star formation rate for galaxies with stellar mass, $M_* > 10^{11} M_\odot$ is $\langle \psi \rangle = 103 \pm 8 M_\odot \text{ yr}^{-1}$ (Bauer et al. 2011), with a dispersion of $75 M_\odot \text{ yr}^{-1}$. We find very similar star formation rates for the same sample when we examine their *Herschel* far-infrared spectral energy distributions (Hilton et al. 2012). We furthermore measure the star formation rate for galaxies at a constant co-moving merger adjusted

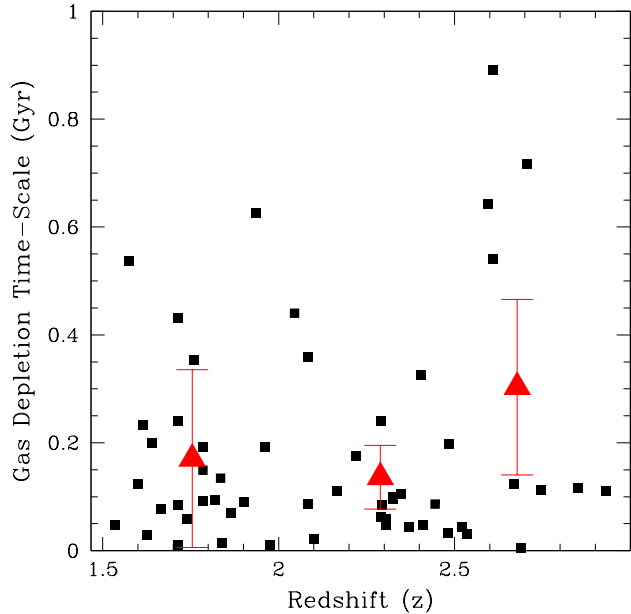


Figure 4. The gas depletion time scale shown as a function of redshift for each galaxy within our sample. The time-scale is in Gyr, and the triangles show the average values at different redshift ranges, and the errors bars are the 1σ scatter.

number density at lower redshifts, from our initial sample. When we do this we find that the star formation rate remains at near $100 M_\odot \text{ yr}^{-1}$, with a slight decline from $110 M_\odot \text{ yr}^{-1}$ to $100 M_\odot \text{ yr}^{-1}$ over the interval $1.5 < z < 3$. We use this star formation rate history at a constant merger adjusted co-moving number density when calculating the formation history of our initial sample of $M_* > 10^{11}$ galaxies.

The observations we use in this paper are measured from redshifts $z = 3$ to $z = 1.5$, a time period of roughly 2.16 Gyrs. We calculate how much stellar mass is created during this redshift interval by integrating the star formation rate, $(\int \psi \times \delta t)$. We also account for mass loss due to stellar evolution processes which we denote as $M_{*,\text{recy}}$. When we do this, we obtain the average amount of stellar mass created per galaxy over this redshift interval, the value of which is: $(\int \psi \times \delta t) \sim (2.24 \pm 0.34) \times 10^{11} M_\odot$. This is roughly the average amount of stellar mass originally in our sample of galaxies at our highest redshift, $z \sim 2.75 - 3$, which we denote as $M_*(t=0) = M_*(0)$.

The term $(M_{*,\text{recy}})$ accounts for the amount of stellar matter brought back into the interstellar medium of these galaxies due to SN, and other stellar evolutionary events using Bruzual and Charlot (2003) models. Using a constant star formation model, which matches the observations, we obtain the net amount of stellar mass created after considering the amount brought back into the ISM through these process, using a Salpeter IMF. We find that on average this amounts to 18% of the stellar mass in star formation is brought back to the ISM of each galaxy. An integral of this is done over our time-span from $1.5 < z < 3$ and the

resulting amount of stellar mass converted back into gas is denoted as $M_{*,\text{recy}}$.

Thus we can measure the ratio of the net stellar mass created in star formation within these galaxies divided by the original stellar mass within these systems, or,

$$\frac{(\int \psi \times \delta t) - M_{*,\text{recy}}}{M_*(0)} = 1.00 \pm 0.15.$$

This is then the amount of gas mass converted into stars due to the star formation process which remains after stellar evolutionary effects have been accounted for at a constant merger adjusted co-moving number density.

3.3 The Evolution of Stellar Mass from Minor+Major Mergers

When calculating the accretion of stellar mass into our sample of galaxies, we have to consider both major and minor mergers, as another major route for galaxies obtaining stellar mass. The amount of stellar mass added to a galaxy due to the merger process is given by the integral over the merger history, based on the fraction of galaxies merging, and the time-scale for mergers (e.g., Conselice et al. 2003; Conselice 2009; Bluck et al. 2009; 2012). We carry out this integration using the observed merger history and time-scale for mergers measured directly from our sample (e.g., Bluck et al. 2009; 2012).

As detailed in Bluck et al. (2012) the merger fraction can be parameterised as a function of both stellar mass and redshift. Bluck et al. (2012) find that at $2.3 < z < 3$ the merger fraction dependence on stellar mass for galaxies within our stellar mass range is given by:

$$f_m(M_*) = (0.28 + / - 0.17) \times \delta \log(M_*)^{0.91 + / - 0.35} \quad (2)$$

and at $1.7 < z < 2.3$ Bluck et al. (2012) find the merger fraction for the same co-moving number density of galaxies is:

$$f_m(M_*) = (0.16 + / - 0.11) \times \delta \log(M_*)^{1.18 + / - 0.35}. \quad (3)$$

The total amount of stellar mass accreted is then a double integral over the redshift range of interest and over the stellar masses which we probe, which for the GNS is sensitive down to $M_* = 10^{9.5} M_\odot$, can be written as,

$$M_{*,M} = \int_{z_1}^{z_2} \int_{M_1}^{M_2} M_* \times \frac{f_m(z, M_*)}{\tau_m} dM_* dz. \quad (4)$$

Where τ_m is the merger time-scale, which depends on the stellar mass ratio of the merging pair (Bluck et al. 2012). The value of τ_m ranges from 0.4 Gyr for a 3:1 stellar mass ratio merger, 1 Gyr for a 9:1 stellar mass ratio merger based on N-body/hydrodynamical simulations, while even higher mass ratios can be even longer with a logarithmic dependence on mass ratio (see Bluck et al. 2012 for details). Our total integration gives a value of

$$\frac{M_{*,M}}{M_*(0)} = 0.56 \pm 0.15.$$

This is the amount of stellar mass added due to both major and minor mergers for systems with stellar mass ratios down to 1:100 for the average system in our sample. After taking

into account baryonic mass, this reduces to mass ratios of 1:20. We cannot extrapolate this to lower mass ratios easily as we have no data on the lower mass merger fractions, but down to $\log M_* = 8.5$ we would add a small amount of mass, but the merger time-scales for these extremely low mass mergers is likely much too long to have merged by $z = 1.5$ (e.g., Bluck et al. 2012).

We integrate the amount of gas mass added due to mergers in a similar way, based on the ratio of stellar to gas mass, based on the data shown in Figure 2. We fit an empirical relationship between the gas mass fraction μ_{gas} and the stellar mass, finding

$$\mu_{\text{gas}} = -0.35 \times \log M_* + 4.13.$$

This relation allows us to compute the total amount of gas, and the total amount of stellar mass accreted from these minor mergers. We show in Figure 5 the relative amounts of gaseous and stellar mass as a function of the stellar mass of the merging galaxy. This shows that the contribution of stellar mass to an average massive galaxy in our sample from merging systems is highest around $M_* = 10^{10.8} M_\odot$ and declines at lower and higher masses. The gas mass accreted however is quite low at the highest mass galaxies, but increases at lower masses and stays relatively constant at values $M_* < 10^{10.5} M_\odot$.

Using this, we calculate how much gas mass is brought into our galaxies due to these minor mergers. We calculate that the average stellar mass weighted gas mass fraction is $f_g \sim 1.03$ down to $M_* = 10^{9.5} M_\odot$. From this, we find $M_{g,M}/M_*(0) = M_{*,M}/M_*(0) \times f_g = 0.57 \pm 0.15$. We assume here that the relation between gas density and stellar mass is constant over the redshift interval $1.5 < z < 3$. We find this to be the case for our massive galaxies, and if the gas within the lower mass galaxies declined at lower redshifts, we would only need more gas accretion to account for the observed star formation, making our measurement a lower limit in this sense. This gas contribution from the minor mergers is our key new measurement that allows us to later constrain how much gas is coming from the intergalactic medium to form galaxies.

4 GAS ACCRETION

4.1 Formulation of Problem

A galaxy has several mass components that interlink with each other. These are the stellar mass (M_*), cold gas mass (M_g) and dark matter mass. For the purposes of this paper we consider that the gas mass is cold, and thus any hot gas or gas that cannot be converted into stars quickly is not included here. Hot gas is present within massive galaxies at least in the local universe, and it remains possible that some of this hot gas is cooling to form stars within the systems we observe here. What we are interested in is the amount of new cold gas which arises from either gas accretion from the intergalactic medium or from hot gas within the halos of these galaxies cooling, which remains a theoretical possibility (e.g. Keres et al. 2005; Ocirk et al. 2008). Our method is ultimately not able to distinguish between these possibilities.

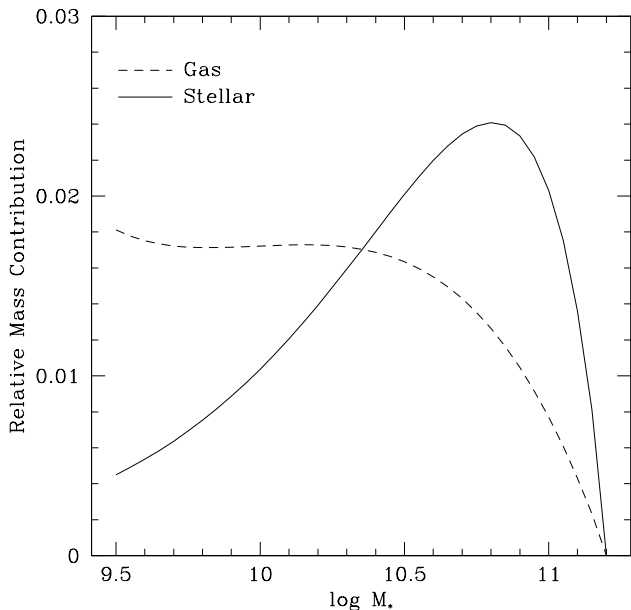


Figure 5. The relative amount of gaseous and stellar matter accreted from mergers of various masses between redshifts $1.5 < z < 3$. The x-axis is the stellar mass of galaxies merging with our typical average galaxy from our sample with $M_* = 10^{11.2} M_\odot$. The y-axis shows the relative contribution to the total for galaxies at masses separated by 0.05 dex. The solid line shows the stellar mass contribution and the dashed line the gaseous contribution.

The total baryonic mass (M_{bary}) of a galaxy can be written as:

$$M_{\text{bary}} = M_* + M_g \quad (5)$$

where these terms are all expressible as a function of time. We first calculate using these terms the amount of stellar mass within a galaxy as a function of time $M_*(t)$. As the stellar mass in a galaxy will not significantly decrease, the value of M_* can in general only increase. This increase can occur through the accretion of outside material from mergers ($M_{*,M}(t)$), and through star formation. We write the increase due to star formation as $\int \psi \times \delta t$, where ψ is the star formation rate within the galaxy as a function of time (§3.2).

We then write the change of stellar mass as a function of time, $M_*(t)$, as

$$M_*(t) = M_*(0) + M_{*,M}(t) + \int \psi \times \delta t - M_{*,\text{recy}}, \quad (6)$$

where $M_*(0)$ is the initial galaxy stellar mass at $t = 0$, and $M_{*,\text{recy}}$ is the amount of stellar mass in stars which is converted back into a gaseous form due to stellar evolution (§3.2).

We further express how the cold gas mass (M_g) changes in a similar way, although the cold gas mass can increase or decrease with time depending on the star formation and gas accretion rate.

$$M_g(t) = M_g(0) + M_{g,M}(t) + M_{g,A}(t) - \int \psi \times \delta t + \epsilon M_{*,\text{recy}} \quad (7)$$

where in this case we have a term for the amount of cold gas brought in from mergers, $M_{g,M}(t)$, the amount from accretion of gas without other galaxies¹, or cold gas accretion, $M_{g,A}(t)$, as well as the amount of gas returned to the interstellar medium from stellar evolution processes. Furthermore the ongoing star formation within this fiducial system will lower the amount of cold gas over time by the amount $-\int \psi \times \delta t$. Some of the mass created in star formation will be returned to the ISM ($M_{*,\text{recy}}$), and only a fraction $\epsilon = 0.001$ of that mass can be reprocessed into stars, as most of the gas is shock heated and thus cannot be used again in star formation in a time scale of a few Gyr (Bruzual & Charlot 2003). We carried out new calculations with different star formation histories showing that even with a higher ϵ not much stellar mass is created from this new gas.

One of the observations of our sample which we described in §3.1 is that the gas mass fraction, M_g/M_* is roughly constant over the interval $1.5 < z < 3$ (e.g., Erb et al. 2006; Genzel et al. 2010). In this case, we can write

$$\frac{M_g(t)}{M_*(t)} \sim \frac{M_g(0)}{M_*(0)}, \quad (8)$$

which is the case in the redshift range we examine for our co-moving constant merger adjusted number density. Note that by using this condition the actual value of the gas to stellar mass ratios is immaterial for the following derivation. Thus, if we use a different relation between star formation surface density and gas surface density we would obtain the same results for the basic equations, although the final numerical result may differ (§4.2). We later examine how our net results would change if there was an evolution such that the gas mass surface density declined at lower redshifts (§4.3).

Using this measurement, we then write the amount of gas mass at a later time t , $M_g(t)$ by using equation 8. We then expressing the stellar mass evolution with time by using equation 6 to replace $M_*(t)$ from equation 8 to obtain

$$M_g(t) = M_g(0) \times \left(1 + \frac{M_{*,M}(t)}{M_*(0)} + \frac{\int \psi \times \delta t - M_{*,\text{recy}}}{M_*(0)} \right), \quad (9)$$

where the gas mass evolution is expressed in terms of the initial gas mass and as a function of how much relative mass is added to a galaxy over time due to the increase from star formation and the increase from mergers. These are much easier to determine than the corresponding absolute amounts (§3).

Therefore using equation (9), and the results presented in §3, we can write the total gas mass after a time δt with respect to the initial gas mass, $M_g(0)$ as

$$M_g(t) \sim (2.56 \pm 0.21) \times M_g(0), \quad (10)$$

such that the total gas mass within our galaxies at $z \sim 1.5$ must be on average ~ 2.56 times larger than the gas mass at the start of our redshift epoch near $z \sim 3$ due to the increase in stellar mass.

¹ Note that this is not strictly true, as this gas in principle could arise from extreme minor mergers, those with mass ratios which are less to 1:100 and which we are not sensitive to in our observations (Bluck et al. 2012). However, the total amount of gas needed implies that these extreme minor mergers would vastly outnumber the visible minor mergers at a level much higher than any reasonable extrapolation.

If we then equate this to equation (7) we can calculate that the accreted (or extra) gas mass is given by:

$$\dot{M}_{g,A}(t) = (1.56 \pm 0.21) \times \dot{M}_g(0) + \int \psi \times \delta t - \epsilon \dot{M}_{*,\text{recy}} - \dot{M}_{g,M}(t). \quad (11)$$

If we divide this equation by the average initial stellar mass $M_*(0)$ we get:

$$\frac{\dot{M}_{g,A}(t)}{M_*(0)} = (1.56 \pm 0.21) \times \frac{\dot{M}_g(0)}{M_*(0)} + \frac{\int \psi \times \delta t - \epsilon \dot{M}_{*,\text{recy}}}{M_*(0)} - \frac{\dot{M}_{g,M}(t)}{M_*(0)}. \quad (12)$$

Therefore by knowing the initial average gas mass fraction, the fraction of stellar mass increase in the form of stars, and the gas mass fraction brought in through merging, we can determine the amount of gas mass, relative to our average galaxy's initial stellar mass, brought in through 'pure' accretion events, i.e., not gas brought in with merging galaxies.

4.2 Gas Accretion Mass Fraction

As we discuss in §3.1 we find that the initial gas mass fraction at $z = 3$ is $f_g = 0.17 \pm 0.06$, $\sigma = 0.19$, and that the fraction of stellar mass formed in star formation after accounting for stellar evolution is $= 1.00 \pm 0.15$ (§3.2), and the amount added from mergers is $M_{*,M}/M_*(0) = 0.56 \pm 0.15$ (§3.3). The most difficult value to determine is the ratio of the cold gas mass brought in from mergers to the total amount of initial stellar mass ($\dot{M}_{g,M}(t)/M_*(0)$). However, we are able to make a measurement of this based on the amount of mass accreted from mergers ($\dot{M}_{g,M}$) and the mass weighted gas mass fraction for these systems f_g from §3.3.

We now use the above values, the results from §3, and equation (12) to calculate the amount of gas accreted as a fraction of the initial stellar mass. Putting these together, we conclude that

$$\frac{\dot{M}_{g,A}}{M_*(0)} = 0.70 \pm 0.22. \quad (13)$$

This implies that a roughly constant gas mass fraction seen in the observations of these distant galaxies (§3.1) reveals that on order the entire initial stellar mass of a massive galaxy is added over time, outside of mergers, to form stars during $1.5 < z < 3$. This equates to an absolute amount of gas accreted as $(1.3 \pm 0.41) \times 10^{11} M_\odot$ over 2.16 Gyr, or at an average rate of gas accretion of

$$\frac{dM_{g,A}(t)}{dt} = \dot{M}_{g,A} = (61 \pm 19) M_\odot \text{ yr}^{-1}, \quad (14)$$

needed to produce the star formation we observe. This is the amount of accreted gas which is directly used to form stars within these massive galaxies. This is however the net amount of gas which is accreted. What we have not considered yet is the effects of outflows from galaxies which will remove some fraction of the gas which is accreted. The result of these outflows is that the gross amount of gas actually accreted is the combination of the outflowing gas as well as the gas used in star formation. This in principle could easily double the amount of gas mass needed to be accreted from the IGM (e.g., Faucher-Giguere et al. 2011).

It is now well established that outflows from galaxies, particularly star forming galaxies, are present in observations (e.g., Heckman et al. 2000; Pettini et al. 2000; Weiner

et al. 2009). These papers show that the velocity of the outflow is proportional to the star formation rate (SFR) such that $V \sim \text{SFR}^{0.35}$, where there is a mild increase in the velocity of the outflow with higher star formation rate.

Weiner et al. (2009) measured the velocity outflows and rates for galaxies up to $z \sim 1.5$ in the DEEP2 survey. They calculate that the mass outflow rate, \dot{M}_{outflow} can be expressed as,

$$\dot{M}_{\text{outflow}} = 22 M_\odot \text{ yr}^{-1} \left(\frac{N_H}{10^{20} \text{ cm}^{-2}} \right) \left(\frac{R}{5 \text{ kpc}} \right) \left(\frac{v}{300 \text{ km s}^{-1}} \right).$$

Where in this equation N_H is the column density of gas, estimated by Weiner et al. (2009) for massive galaxies to be $N_H = 1.3 \times 10^{20} \text{ cm}^{-2}$, R is the radius of an expanding shell model of gas, and v is the velocity of outflows. For our star forming galaxies we find a velocity average from Weiner et al. (2009) just over 300 km s^{-1} . Combining this with typical Petrosian sizes for these systems, as a measure of the minimum covering fraction, we obtain an outflow rate of $\dot{M}_{\text{outflow}} = 35 M_\odot \text{ year}^{-1}$ which should be added to the net gas inflow rate that is converted into stars. Therefore we obtain a gross inflow rate which is

$$\dot{M}_{\text{acc}} = \dot{M}_{\text{outflow}} + \dot{M}_{g,A} = 96 M_\odot \text{ yr}^{-1},$$

In the next section we evaluate the uncertainties within this measurement, and in the section after give the implications of this result.

4.3 Uncertainties

There are systematic issues that could affect these results, some of which we examine in this section. One of these is that the the star formation surface density-gas surface density relation (Schmidt-Kennicutt law) may evolve (e.g., Daddi et al. 2010). Since starbursts are more efficient, the initial gas mass could in principle be lower than what we are measuring. If the normal Schmidt-Kennicutt law then applied for the lower redshift galaxies in our sample the net result would be an *increase* in the gas mass to stellar mass ratio and equation 8 no longer strictly holds. Likewise, it may be possible that we are measuring the gas masses incorrectly too low at our highest redshift point for some reason and that there is actually a decrease with time in the gas mass fraction. We examine both of these scenarios quantitatively by considering how our relations would change if we use a gas mass surface density relation of the form:

$$\frac{\dot{M}_g(t)}{M_*(t)} \sim \kappa(t) \times \frac{\dot{M}_g(0)}{M_*(0)}, \quad (15)$$

where $\kappa(t)$ is the relative change in the ratio between the gas to stellar mass at some lower redshift than at the initial time at $z \sim 3$. In this case, the relative gas mass accretion can be written as:

$$\frac{\dot{M}_{g,A}(t)}{M_*(0)} = \kappa \times 1.56 \times \frac{\dot{M}_g(0)}{M_*(0)} + \frac{\int \psi \times \delta t}{M_*(0)} - \frac{\dot{M}_{g,M}(t)}{M_*(0)} - \frac{\epsilon \dot{M}_{*,\text{recy}}}{M_*(0)}. \quad (16)$$

When using this equation with the value of $\kappa = 0.5$, where the gas mass fraction has dropped by a half, we find that the gas accretion mass fraction drops to $\dot{M}_{g,A}/M_* = 0.56 \pm 0.22$. If we take the limiting case where all of the gas is exhausted

from $z = 3$ to $z = 1.5$, where $\kappa = 0$, we would find a lower limit accreted gas mass fraction of $M_{g,A}/M_* = 0.43 \pm 0.22$.

In general, if the gas mass fraction decreases with time, with perhaps an evolving form of the relation between gas mass surface density and star formation rate surface density, this would result in a slightly lowered derived gas mass accretion. For the more likely case of less efficient star forming systems over time, the net gas mass fraction would increase even more than our initial calculation, given that in this case $\kappa > 1$. However, most of the constraint on this measurement comes from the fact that there is a high ongoing star formation rate during this epoch, and the gas to fuel this star formation is not initially present within the galaxy, nor carried in through mergers.

If we directly consider the more efficient Schmidt-Kennicutt law, as proposed by Daddi et al. (2010) for star bursting galaxies to apply throughout our redshift range, we would then have a lower gas mass fraction at both the start and the end of our evolution. As above, we would still have to account for the star formation present within these systems, and this is the driving observation behind our calculation of a high gas mass accretion rate. However it is important to note that our galaxies are in the regime where they follow the standard law (Daddi et al. 2010), where the more efficient starburst are found within sub-mm and ULIRG galaxies (Figure 2).

One remaining issue is that our star formation rates maybe too high, however, others have found very similar star formation rates or higher, for similar galaxies (e.g., Daddi et al. 2007). The star formation rates we measure are consistent in the ultraviolet and using *Herschel* far-infrared imaging (Hilton et al. 2012), and if anything our values are at the lower end of the various star formation measurements (Bauer et al. 2011).

4.4 Implications

We present in this paper an analysis of the amount of cold gas mass which is likely accreted into massive galaxies with stellar masses $M_* > 10^{11} M_\odot$ at $1.5 < z < 3$. This amount of accreted gas is necessary to account for the observed star formation rate between redshifts $1.5 < z < 3$, which cannot be accounted for by gas brought in through minor+major mergers (Bluck et al. 2012). Our overall result is that we find a basic accretion rate of $\dot{M}_{g,A} = (96 \pm 19) M_\odot \text{yr}^{-1}$ of cold gas needed from the IGM to account for this star formation. This accounts for $66 \pm 20\%$ of the gas brought into these galaxies and ultimately responsible for $49 \pm 20\%$ of the stellar mass assembly produced between $1.5 < z < 3$. In addition to this we find that $25 \pm 10\%$ of the stellar mass accreted is from mergers, while the remaining $\sim 25\%$ is from star formation produced in gas accretion associated with mergers. Therefore the bulk of the formation of massive galaxies at $1 < z < 3$ is due to conversion of baryons into gas as observed in the star formation rate.

Overall this implies that gas accretion into massive galaxies at early epochs is a major formation method, and may dominate over mergers as a formation process for new stars. We also note that we are not certain what is the origin of this gas accretion. It could originate from cold filaments, or from gas cooling from the halo itself (e.g., Keres et al.

2005; Ocvirk et al. 2008), and we are not able to address this directly.

Papovich et al. (2011) measure the total gas accretion rate at similar redshifts, which includes all methods that bring in gas. They were not able to distinguish between the gas brought in through mergers, and that brought in through gas accretion. Their results are similar to ours, finding a higher accretion rate, but that the total accretion is similar to what we find here, or slightly higher as it includes gas brought in through minor mergers. We note that we are only able to probe mergers for massive galaxies down to $M_* = 10^{9.5} M_\odot$, and it is possible that the gas accretion we find originates from galaxies with stellar masses lower than this limit. Furthermore, we are not able to say whether the accreted gas originates in clumps of gas into the galaxy or in a smooth continuous mode. We also cannot rule out that some of this gas is originating from the outer halo after cooling. Our result is an integrated average of gas accretion through these modes over the time-spanned by redshifts $1.5 < z < 3$.

There are several implications from these results. Our finding may explain how some massive galaxies in the very local universe, outside the Local Group but within 8 Mpc, can have almost no bulges (e.g., Kormendy et al. 2010). Gas accretion is also one way to solve the G-dwarf problem of having too many metal rich stars in the solar neighbourhood (e.g., Larson et al. 1974), and may relate to the gas accretion we see in our own galaxy (Blitz et al. 1999).

Overall our result of finding an accretion rate of gas of $\dot{M}_{\text{acc}} = (96 \pm 19) M_\odot \text{yr}^{-1}$ for the most massive galaxies at $1.5 < z < 3$ is roughly consistent with theoretical calculations which predict a similar amount of gas accretion (Murali et al. 2002; van den Bosch 2002; Keres et al. 2005; Dekel et al. 2009a,b). Early simulations by Murali et al. (2002) predict a gas accretion rate of $\dot{M}_{g,A} \sim 40 M_\odot \text{yr}^{-1}$, while more recent work suggests higher rates of $\dot{M}_{g,A} \sim 100 M_\odot \text{yr}^{-1}$ (e.g., Dekel et al. 2009a,b; Faucher-Giguere et al. 2011). Our results are in general agreement with these models, although we are only examining a narrow redshift and stellar mass interval within this paper.

Our results from this work, and previous papers examining the issue of stellar mass formation modes (e.g., Conselice 2006; Bluck et al. 2012) is similar to what is predicted in several studies using N-body simulations. This includes Genel et al. (2010), who find through simulations that about 60% of the dark matter mass in galaxies is put into place through merging, with at least 40% of the mass coming from accretion. This is however, for the formation of the dark matter halo and not the baryons or stars. Using hydrodynamical galaxy formation models, Murali et al. (2002) find that for galaxies brighter than about a fourth of L^* , the characteristic luminosity, gas accretion dominates over merging as a mechanism, whereby gas accretion accounts for $\sim 75\%$ of the stellar mass build up at $z \sim 2$. While others, e.g., Stewart et al. (2008) find that over half of the mass in galaxies is formed in mergers, while others such as Angulo & White (2010) find that nearly all the mass in galaxies is put into place via mergers. Finally Keres et al. (2009) find that the minor+merger mass assembly is comparable to the formation due to gas accretion. There is therefore considerable disagreement between these various models about which mode is the dominant. We find that the gas accretion and merg-

ers are about as equally important. Future studies will have to probe deeper to obtain the merger history for lower mass systems to carry out similar calculations as these, and probe this evolution in different environments.

5 SUMMARY

We present in this paper a study of the cold gas mass densities for massive galaxies with $M_* > 10^{11} M_\odot$ at redshifts of $1.5 < z < 3$. While we do not directly detect the accretion of gas within our galaxies, we are able to make a circumstantial finding for its existence. Our conclusions are as follows:

I. Utilizing our measured star formation rates and galaxy sizes we find a roughly constant cold gas mass to stellar mass fraction for this sample across the redshift range of $1.5 < z < 3$.

II. We utilize the star forming and merging properties of these galaxies from previous work in Bauer et al. (2011) and Bluck et al. (2012) to measure the mass budget of our sample of massive galaxies, finding that $\dot{M}_{\text{acc}} = (96 \pm 19) M_\odot \text{ yr}^{-1}$ of gas is needed to sustain the star formation rate outside of gas brought in via mergers.

III. We derive based on these values that cold gas accretion from the intergalactic medium, or alternatively very minor galaxy mergers with mass ratios lower than 1:100 (or 1:10 in ratios of baryons), accounts for $49 \pm 20\%$ of the baryonic matter added to galaxies from $1.5 < z < 3$.

This amount of gas mass added from accretion is larger than the amount of gas added due to the merger process (both minor and major) (e.g., Conselice 2006; Bluck et al. 2012) and is largely in agreement with models which predict on the order of $100\text{--}200 M_\odot \text{ yr}^{-1}$ added from cold gas accretion (e.g., Dekel et al. 2009a,b). Gas accretion is therefore the major method for producing star formation within massive galaxies between redshifts $1.5 < z < 3$.

Further work with e.g., the CANDELS survey will allow us to carry out this measurement for lower mass galaxies where the mode of formation could be significantly different than the more massive systems (e.g., Dekel et al. 2009a,b). Also, we are examining in this paper massive systems in the last throws of their formation at $z < 3$. Investigating the ratio of formation due to mergers and gas accretion at $z > 3$ will reveal how the first epochs of these massive galaxies were formed. This however will require observations from JWST and the ELTs.

We thank the GNS team, particularly Fernando Buitrago and Amanda Bauer, for their contributions to this survey and the previous published work utilised here. We thank the referee for a report that improved this paper significantly. The data and catalogs as used in the GNS survey are online at: <http://www.nottingham.ac.uk/astronomy/gns/>.

The GNS is financially supported by STFC and the Leverhulme Trust. Support was also provided by NASA/STScI grant HST-GO11082.

REFERENCES

Angulo, R.E., White, S.D.M. 2010, MNRAS, 401, 1796

- Bauer, A.E., Conselice, C.J., Perez-Gonzalez, P.G., Gruzbauch, R., Bluck, A.F.L., Buitrago, F., Mortlock, A. 2011, MNRAS, 417, 289
- Bigiel, F., et al. 2011, ApJ, 730, 13L
- Birnboim, Y., Dekel, A. 2003, MNRAS, 345, 349
- Blitz, L., Spergel, D.N., Teuben, P.J., Hartmann, D., Burton, W.B. 1999, ApJ, 514, 818
- Bluck, A., et al. 2009, MNRAS, 394, 51L
- Bluck, A., et al. 2012, MNRAS, 417, 34
- Boquien, M., Lisenfeld, U., Duc, P.-A., Braine, J., Bournaud, F., Brinks, E., Charmandaris, V. 2012, A&A, 539, 145
- Bouche, N., et al. 2007, ApJ, 671, 303
- Bournaud, F., et al. 2011, ApJ, 730, 4
- Bouwens, R., et al. 2010, ApJ, 725, 1587
- Bruzual, G., Charlot, S. 2003, MNRAS, 344, 1000
- Buitrago, F., Trujillo, I., Conselice, C.J., Bouwens, R.J., Dickinson, M., Yan, H. 2008, ApJ, 687, 61L
- Buitrago, F., Trujillo, I., Conselice, C.J., Conselice, C.J., Haeussler, B. 2011, arXiv:1111.6993
- Bundy, K., et al. 2006, ApJ, 651, 120
- Conselice, C.J., Bershadsky, M.A., Dickinson, M., Papovich, C. 2003, AJ, 126, 1183
- Conselice, C.J., Rajgor, S., Myers, R. 2008, MNRAS, 386, 909
- Conselice, C.J. 2006, ApJ, 638, 686
- Conselice, C.J. 2009, MNRAS, 399, 16L
- Conselice, C.J., et al. 2011, MNRAS, 413, 80
- Dave, R., Oppenheimer, B.D., Finlator, K. 2011, MNRAS, 415, 11
- Daddi, E., et al. 2007, ApJ, 670, 156
- Daddi, E., et al. 2010, ApJ, 714, 118L
- Dekel, A., et al. 2009a, Nature, 457, 451
- Dekel, A., Sari, R., Ceverino, D. 2009b, ApJ, 703, 785
- Erb, D.K., Steidel, C.C., Shapely, A.E., Pettini, M., Reddy, N.A., Adelberger, K.L. 2006, ApJ, 646, 107
- Faucher-Giguere, C.-A., Keres, D., Ma, C.-P. 2011, MNRAS, 417, 2982
- Ferguson, H.C., et al. 2004, ApJ, 600, 107L
- Fumagalli et al. 2011, MNRAS, 418, 1796
- Genel, S., Bouche, N., Naab, T., Sternberg, A., Genzel, R. 2010, ApJ, 719, 229
- Genzel, R., et al. 2008, ApJ, 687, 59
- Genzel, R., et al. 2010, MNRAS, 407, 2091
- Giavalisco, M., et al. 2011, ApJ, 743, 95
- Grützbauch, R., et al. 2011a, MNRAS, 418, 938
- Grützbauch, R., et al. 2011b, MNRAS, 412, 2361
- Heckman, T.M., Lehnert, M., Strickland, D., Armus, L. 2000, ApJS, 129, 493
- Hilton, M., et al. 2012, MNRAS, 425, 540
- Kennicutt, R.C. 1998, ApJ, 498, 541
- Keres, D., Katz, N., Weinberg, D.H., Dave, R. 2005, MNRAS, 363, 2
- Kimm, et al. 2011, MNRAS, 413, L51
- Kormendy, J., Drory, N., Bender, R., Cornell, M.E. 2010, ApJ, 723, 54
- Krumholz, M.R., Dekel, A., McKee, C.F. et al. 2012, ApJ, 745, 69
- Larson, R.B. 1974, MNRAS, 166, 585
- Mannucci, F., et al. 2009, MNRAS, 398, 1915
- McBride, J., Fakhouri, O., Ma, C.-P. 2009, MNRAS, 398, 1858

- Mortlock, A., Conselice, C.J., Bluck, A.F.L., Bauer, A.E., Grutzbauch, R., Buitrago, F., Ownsworth, J. 2011, MNRAS, 413, 2845
- Murali, C., Katz, N., Hernquist, L., Weinberg, D.H., Dave, R. 2002, ApJ, 571, 1
- Narayanan, D., Krumholz, M., Ostriker, E.C., Hernquist, L. 2011, MNRAS, 418, 664
- Ocvirk, P., Pichon, C., Teyssier, R. 2008, MNRAS, 390, 1326
- Ownsworth, J.R., Conselice, C.J., Mortlock, A., Hartley, W., Buitrago, F. 2012, MNRAS, 426, 764
- Papovich, C., Finkelstein, S.L., Ferguson, H.C., Lotz, J.M., Giavalisco, M. 2011, MNRAS, 412, 1123
- Pettini, M., Steidel, C.C., Adelberger, K., Dickinson, M., Giavalisco, M. 2000, ApJ, 528, 96
- Rauch, M., Becker, G.D., Maehnel, M.G., Gauthier, J.-R., Ravindranath, S., Sargent, W. 2011, MNRAS, 418, 1115
- Steidel, C. et al. 2010, ApJ, 717, 289
- Stewart, K.R., Bullock, J., Wechsler, R., Maller, A., Zentner, A. 2008, ApJ, 683, 597
- Tacconi, L. et al. 2010, Nature, 463, 781
- Trujillo, I., Conselice, C.J., Bundy, K., Cooper, M.C., Eisenhardt, P., Ellis, R.S. 2007, MNRAS, 382, 109
- van den Bosch, F. 2002, MNRAS, 331, 98
- Weiner, B., et al. 2009, ApJ, 692, 187
- Weinzirl, T., et al. 2011, ApJ, 743, 87
- White, S.D.M., Frenk, C. 1991, ApJ, 379, 52